

THE NUMBER OF BLADE EFFECTS ON THE PERFORMANCE OF A MIXED TURBINE ROTOR

Litim Sid Ali ^{1*} – Hamel Mohammed ¹ – Hamidou Mohamed Kamel ¹

¹ Department of mechanical engineering, Faculty of mechanical engineering, University of Sciences and Technologies Mohamed Boudiaf of Oran, El Mnaouar, BP 1505, Bir El Djir 31000, Algeria

ARTICLE INFO

Article history:

Received: 14.06.2016.

Received in revised form: 01.12.2016.

Accepted: 06.12.2016.

Keywords:

Mixed Flow Turbine

Performance

Efficiency

Finite Volume Method

ANSYS-CFX

Abstract:

Turbochargers have become widely applied to diesel vehicle engines. The mixed flow turbine type is suitable for systems where compact power sources are required with higher boost pressure. The sensitivity of the rotor to incidence effects and tendency of the flow to separate have given rise to considerations of the optimum number of blades. This paper investigates the performance of a mixed inflow turbine under steady conditions with the effect of the blade number.

This study deals with the determination of the performance characteristics of a mixed flow turbine by solving numerically the 3D Reynolds averaged Navier-Stokes equations. The ANSYS-ICEM software is used to build the geometry and generate the unstructured meshes while the ANSYS-CFX code is used to simulate the flow in the mixed flow turbine.

The numerical method is also used to determine optimum geometrical characteristics such as the optimum number of blades. It has been found that the rotor with 14 blades exhibits better performance.

1 Introduction

Modern diesel engines are fitted with turbochargers in order to increase the output power and reduce pollutant emissions. They were used principally in the early days in the field of marine propulsion and in recent years they became commonly used for road transport applications.

Turbochargers with radial compressors and radial turbines are the most commonly used because of their ability to absorb/deliver more power in comparison to axial ones of similar size. Radial

turbines are mainly used for automotive engine applications and have the advantage of retaining a higher efficiency when reduced to small sizes. They can operate at high expansion ratio on one single stage. On the other hand, axial turbines, which are used for large turbocharger (marine and railway applications) engines, are generally made of several stages. The turbine which is an important component of a turbocharger consists essentially of a casing or volute, a rotor and a diffuser. Radial turbines have been applied to small engine due to their reduced gas emissions, their simplicity,

* Corresponding author. Tel.: +213 667627149

E-mail address: litimsidali@yahoo.fr, sidali.litim@univ-usto.dz

low cost, reliability and relatively high efficiency. The turbine requirements in highly loaded turbocharger engines are changing: higher air/fuel ratio required for fewer emissions and the use of intercoolers result in significantly lower exhaust temperatures. This together with the fact that more power required to boost pressure has to be taken from the exhaust has resulted in using smaller turbine housings, which reduces the turbine efficiency. The turbine speed is limited by stress so that a turbine stage with maximum efficiency at a lower value of blade speed is required. The most feasible way to achieve this is to make the inlet blade angle positive as opposed to the usual value of zero for radial turbines with radial blade fibres. This means that the rotor inlet should not be radial but mixed so that inlet streamlines in the meridian plane have both radial and axial components. It is the only possible way to have non zero inlet rotor blade angle while retaining radial blade fibres. This type of blade geometry with radially directed fibres used for mixed flow rotors has the advantage of avoiding additional stresses due to bending.

Three mixed flow turbines, with rotor A, B and C, have been designed to meet these constraints and then tested at Imperial College by Abidat [1] and Abidat et al. [2]. The two rotors A and C have a 20 degrees constant rotor inlet blade angle and differ only by the number of blades: Rotor A has 12 blades while turbine C has only 10. Rotor B was designed for a notionally constant incidence angle at design conditions. It has the same number of blades and the same exducer geometry as rotor A but shorter axial length. The turbine was designed to match the design conditions presented in Table 1. They found that the rotor with 12 blades has a higher efficiency than the rotor with 10 blades at off design conditions [2].

Table 1. Design conditions

Rotational speed	98000 rpm
Mass flow rate	0.414 kg/s
Total inlet temperature	923 K
Pressure ratio	2.91
Optimum velocity ratio	0.61

This turbine, referred to as turbine A, has been used by Abidat et al. [1,2,3], Arcoumanis et al. [4], Chen et al. [5] and Hamel et al. [6] for steady and unsteady flow performance analyses. Turbine B, on

the other hand, has been investigated by Abidat [1] and Abidat et al. [2] under steady state conditions and by Karamanis et al. [7] under pulsating conditions. Turbine C has been investigated under steady state by Chen et al. [8] in order to investigate the effect of blade loading on the turbine performances. Although, a relatively abundant literature on the performance of radial turbines such as those of Bhinder and Gulati [9], Gabette et al. [10], Dale and Watson [11], Chen and Winterbone [12] and Hammoud et al. [13], is available, more work on mixed flow turbines needs to be done.

A complete review on mixed flow turbines is already made available by Rajoo and Martinez-Botas [14], they provide readers with a comprehensive review of the past and present research into the design, performance, and use of mixed inflow turbines.

Khairuddin et al. [15] describes an optimization procedure to modify the geometry of a mixed inflow turbocharger turbine with 12 blades for improved aerodynamic efficiency. The procedure integrates parameterization of the turbine blade geometry, genetic algorithm optimization, and 3D CFD analysis using a commercial solver. The hub and shroud profiles were observed to have the greatest impact on turbine performance, optimization of which leads to an increase of 1.3 percentage points of efficiency. Nevertheless, Zhang et al. [16] state that the slope of the hub and shroud will have the most influence on turbine performance in the initial design state.

No general methods are available for calculating the optimum number of blades for a given duty. The available methods for calculating the number of blades are empirical and they result in different number of blades for the same geometry [17].

A large number of blades is required for better flow guidance and to avoid flow reversal at the penalty of increased frictional losses and flow blockage. Eventually, a fair compromise solution can be found.

This study presents a numerical performance prediction of the mixed flow turbine for a wide range of rotational speeds, pressure ratios and the blade number effect. The overall geometrical characteristics of the turbine are given in Table 2.

The computational tests are performed with the ANSYS-CFX software on one blade to blade passage (Fig. 3) using the k- ϵ turbulence model. Firstly, the computed results are compared with the

experimental data; secondly, the study of influence of the number of blades on the mixed inflow turbine performance is done.

Table 2. Turbine overall geometrical characteristics

Rotor inlet mean diameter	83.59 mm
Rotor inlet blade height	17.99 mm
Rotor inlet blade angle	20.0 deg
Rotor inlet cone angle	40.0 deg
Exducer hub diameter	27.07 mm
Exducer shroud diameter	78.65 mm
Rotor exit mean blade angle	-52.0 deg
Rotor axial length	40.00 mm
Number of blades	8 to 20
Radial and axial tip clearance	0.4 mm

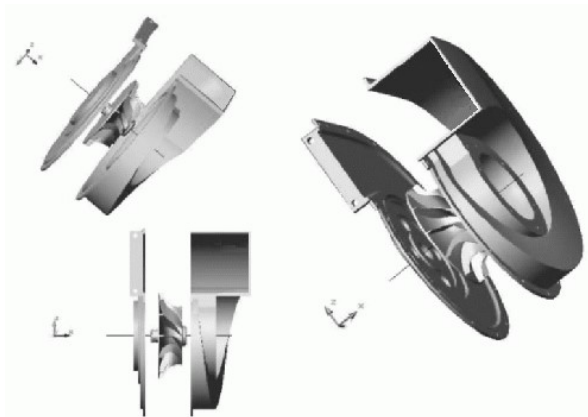


Figure 1. Mixed flow turbine

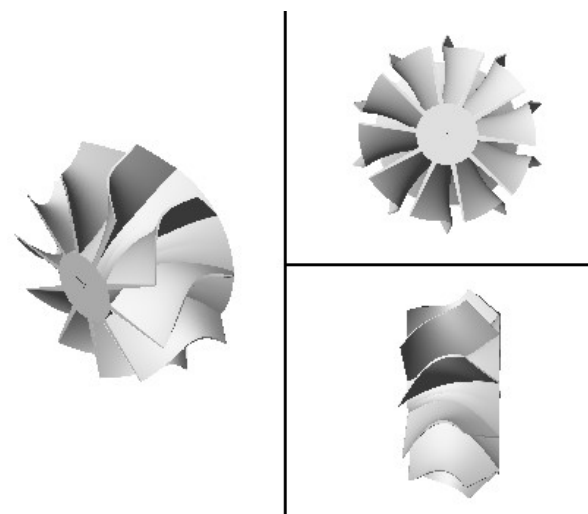


Figure 2. Mixed flow turbine rotor

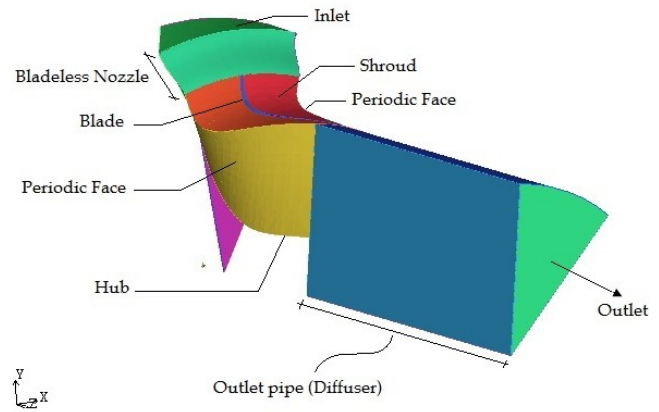


Figure 3. Computational flow domain

2 Numerical method

The highly three dimensional, compressible, viscous and turbulent flow in the mixed inflow turbine shown in Fig. 1, 2 and 3 is obtained by solving numerically the Reynolds averaged equations of mass, momentum and energy conservation. Temperature, pressure and density are related by the equation of state. The turbulence is modeled by the standard k-ε equation of Patankar and Spalding [18]. This model is based on the eddy viscosity concept which assumes that the Reynolds stresses can be expressed in terms of the mean velocity gradients and the turbulent viscosity in a manner analogous to the viscous stresses for laminar Newtonian flows.

2.1 Mesh generation

The flow solution in the mixed inflow turbine, shown in Fig. 3, is obtained by the finite volume approach. The blade channel geometry is built using the ANSYS ICEM CFD software, and then the entire domain is discretized by unstructured mesh of hexahedral elements as shown in Fig. 4.

The influence of the rotational speed exerted on the turbine performance is shown on a one blade to blade channel with periodic flow conditions exhibited on the mean meridian surface. A blade passage including the exhaust pipe is shown in Fig. 3.

During the mesh generation process, care has to be taken in the choice of the first grid spacing near wall boundaries to obtain a proper resolution of the

boundary layer (Fig. 5). As a result of the use of the wall function approach to model the flow near the wall in the $k-\epsilon$ turbulence model, it is advised that the y^+ value for the near wall node has to be in the range of 20 to 100 [19].

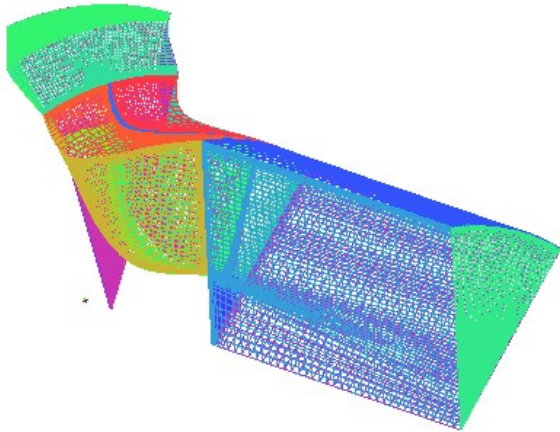


Figure 4. Hexahedral mesh of the blade to blade channel

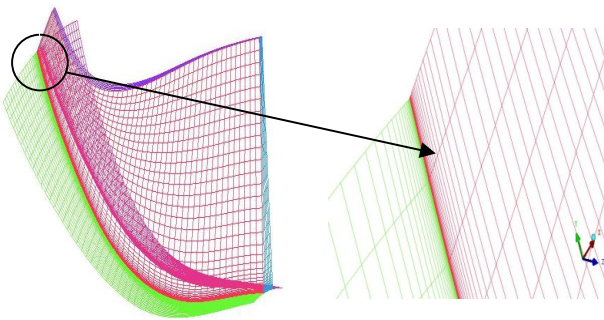


Figure 5. Blade mesh

2.2 Resolution method

The integration on the finite volumes of the equations describing the turbulent flow results in a set of discrete equations. The terms of the differential equations on the volume interfaces are obtained by a second order upwind scheme. The ANSYS-CFX uses a single cell, unstaggered, collocated grid to overcome the decoupling of pressure and/or velocity. The method is similar to that used by Rhie and Chow [20], with a number of extensions, which improve the robustness of the discretization when the pressure changes rapidly, or is affected by body forces. The pressure-velocity coupling is achieved using a coupled solver, which

solves the hydrodynamic equations (for u, v, w, p) as a single system.

At the domain inlet, the flow is assumed to be subsonic, and therefore the total pressure and the total temperature in the stationary frame of reference as well as the flow direction and the intensity of turbulence ($I=5\%$) are imposed. At the turbine outlet, where the flow is considered to be subsonic, the static pressure is imposed. On the solid boundaries, a no slip condition is used. Because of the use of only one blade passage, a periodic boundary condition is assumed at the left and the right of the computational domain (Fig. 3). The conditions of the numerical tests are given in Table 3

Table 3. Numerical test conditions

Rotational Speed (rpm)	Total Inlet Temperature (K)	Pressure Ratio Range
29500 (50%)	333.82	1.218 ~ 1.545
41300 (70%)	333.82	1.445 ~ 2.065
59700 (100%)	341.79	1.902 ~ 3.138

3 Results and discussions

For the first time, the numerical method described in this paper has been used to simulate the effect of the rotor rotational speed and the turbine inlet flow conditions on the performance of a 10 blades mixed inflow turbine. The second time, the model is used to study the effect of blade number on the performance of the mixed inflow turbine without taking into account the effect of the volute on the machine as whole.

As stated by Pullen [21]: tests showed that the presence and speed of the rotor had negligible influence on the volute flow field. The volute accelerates and guides the fluid flow toward the rotor with the optimal entrance angle, uniformity of the thermodynamics parameters, speed and Mach number. The performances of the volute depend on the geometrical shape of the cross-section area single or twin entry, the length, the azimuthal angle and the shape of the tongue. At the end, the selected volute might be matched to the rotor under consideration.

3.1 Grid solution dependency

Four mesh sizes, as given in Table 4, have been used to compute the turbulent flow solution in the mixed flow turbine in order to choose the optimal grid for the final computation. The solutions obtained with the four grids are presented in Fig. 6 in terms of the blade pressure distribution at blade mid span. The grid 02 with 174640 elements was found to give a satisfactory solution and was used for the computation of the test cases presented in Table 3.

Table 4. Mesh size for grid dependency of the solution

Grid	01	02	03	04
Size	116231	174640	287076	383126

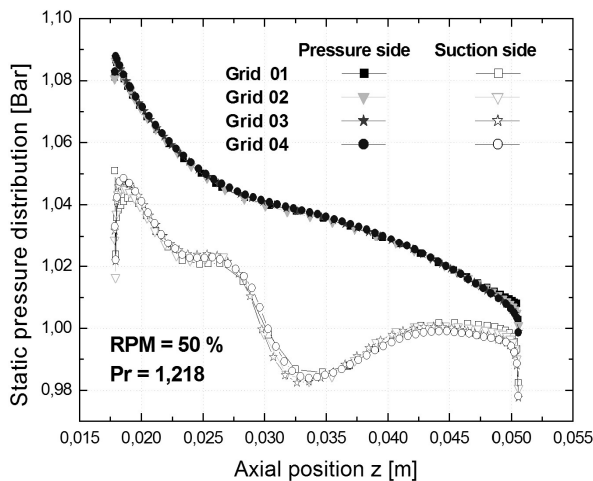


Figure 6. Grid dependency of the solution (50 % Speed, $Pr = 1.218$, $T0^* = 333.82$ K)

A Grid Convergence Index (GCI) is calculated based on Celik et al. [22] method using the calculated mass flow rate as significant variable. The maximum of GCI value is 0.12% indicating that the discretization error has very little influence on the convergence towards the asymptotic solution. For the validation of the numerical model, the numerical results of the 10 blade mixed inflow turbine were compared with experimental data of Abidat et al. [2] for a pressure ratio of 2.5 and a rotational speed of 59700 rpm. Figure 7 shows the variation of the static pressure along the shroud; we note a good agreement of the numerical and experimental results.

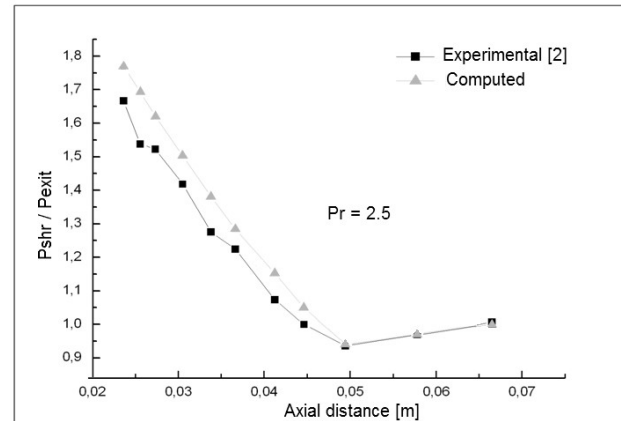


Figure 7. Evolution of the pressure along the shroud ($Pr = 2.5$ and 100% speed)

3.2 Performance characteristics

Figures 8 to 10 show the influence of the rotational speed on the performance characteristics of the turbine. Figure 8 shows the computed mass flow rate characteristics in terms of pressure ratio versus the reduced mass flow rate defined as:

$$Pr = P_{0^*} / P_{exit} \quad (1)$$

$$\dot{m}_r = 10^5 \dot{m} \sqrt{T_{0^*}} / P_{0^*} \quad (2)$$

A satisfactory agreement between the computed and the measured result is observed.

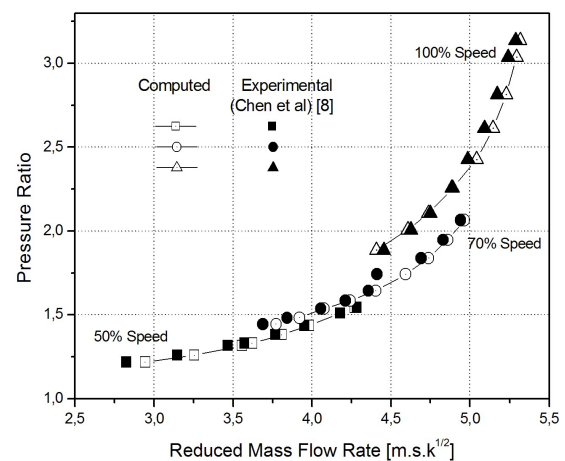


Figure 8. Reduced mass flow rate characteristics

The computational domain shown in Fig. 3 does not include the scroll (volute) part of the turbine stage. In order to compare the computed and the

experimental results for the static to total efficiency (Eq. 3), it was necessary to assess the contribution of the volute in the drop of the overall turbine efficiency.

$$\eta_{TS} = \frac{h_{in^*} - h_{out}}{C_p \cdot T_{in^*} \cdot [1 - (P_{out} / P_{in^*})]^{(\gamma-1)/\gamma}} \quad (3)$$

The resulting total to static efficiency characteristics are presented in Fig. 9. The computed efficiency is slightly overestimated in comparison to the experimental one.

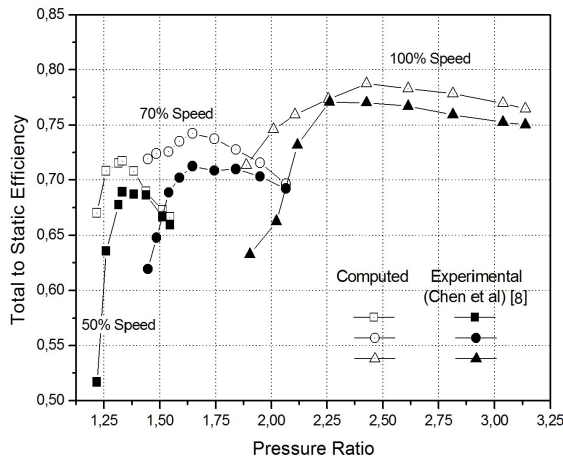


Figure 9. Total to static efficiency vs. pressure ratio

Although a reasonable agreement is obtained at each rotational speed for high pressure ratios, the turbulent flow model used in this computation fails to predict the correct efficiency at lower ones. This deflection can be attributed to the $k-\epsilon$ turbulence model used in this simulation. It is worth mentioning that the $k-\epsilon$ models like other two-equation models, which are suitable for many flows of engineering interest, become limited in applications with boundary layer separation and flows with sudden changes in the mean strain rate, such as those encountered in a turbomachine. The location of the maximum efficiency depends on the rotational speed. A higher efficiency is obtained for the design rotational speed.

3.3 Flow analyses

The distribution of the static pressure and the speed vectors at different pressure ratios and rotational speeds are shown in Fig. 10 to 15.

The blade loading is illustrated by the static pressure contours around the pressure and suction sides of the blade. The blade geometry generates the pressure gradient between the suction and pressure sides, resulting in the torque transmitted to the blade.

These figures confirm that the flow velocities on the suction side are higher than the velocities on the pressure side.

Note that for low speeds and for all pressure ratios, there is always a depression zone at the suction side (Fig. 10 and 11), as predicted, this depression reflects the presence of recirculation which is due to the pressure gradient. This recirculation for such rotational speed is almost stationary except for the small pressure ratios; this explains the sensitivity of the flow at low rotation speeds and low pressure ratios.

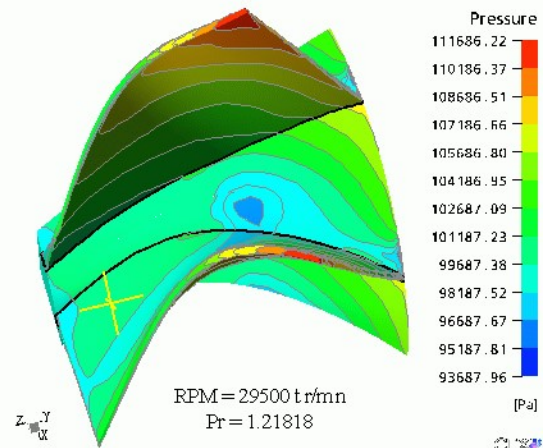


Figure 10. Pressure contours at 50% of speed

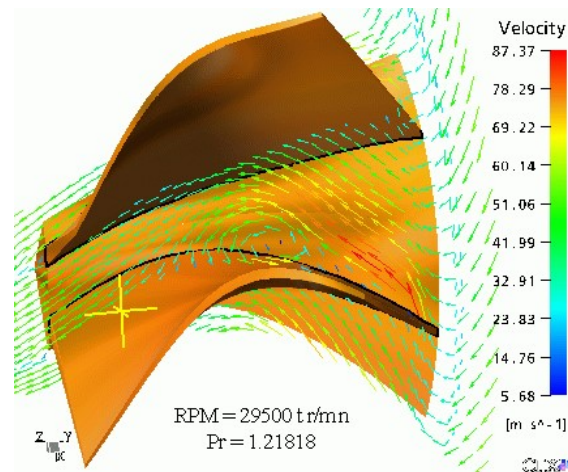


Figure 11. Velocity vectors at 50% of speed

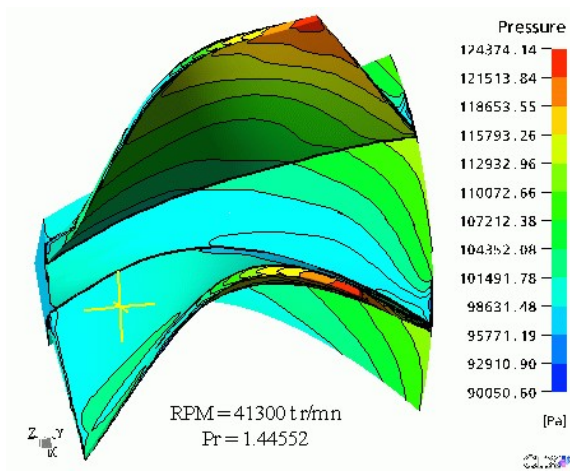


Figure 12. Pressure contours at 70% of speed

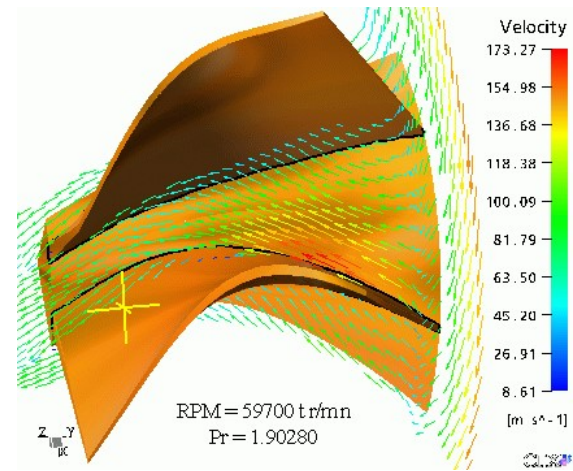


Figure 15. Velocity vectors at 100% of speed

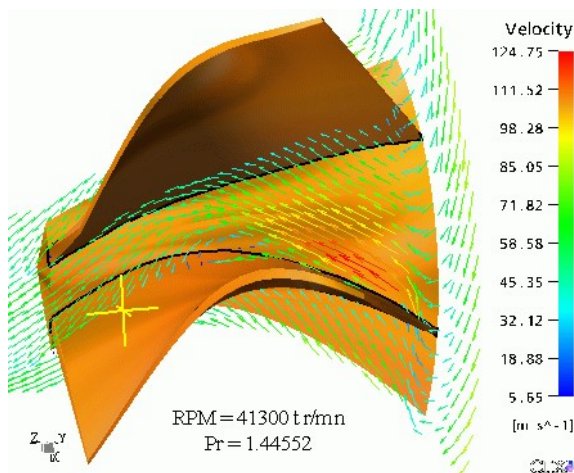


Figure 13. Velocity vectors at 70% of speed

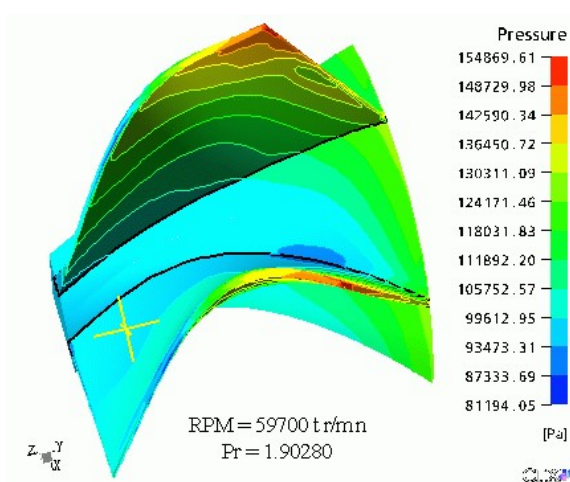


Figure 14. Pressure contours at 100% of speed

We can notice that the recirculation zone tends to disappear when increasing the rotational speed and the pressure ratio (Fig. 12 and 13) until it vanishes completely when 100 % of the rotational velocity is obtained (Fig. 14 and 15), which might justify the increase of the total to static efficiency.

The flow analysis was carried out on 10, 12, 14, 16 and 18 of the turbine blades.

Figures 16 to 25 clearly show the pressure distribution along the blade passage at the surface of the hub and on a hub parallel plane. The distribution is also shown for the pressure at suction sides. We find that with the 10 blade turbine there is a depression area confirming the existence of the recirculation zone. We note that as the number of blades increases, this depression tends to disappear. It can be observed that when the fluid is flowing further down along the blade passage, it expands smoothly through the rotors. It reveals that there is a large pressure gradient across the rotor inlets with higher pressure occurring at the shroud. This pressure gradient is necessary to balance the difference in centrifugal force between the shroud and hub, resulting from the change of radius. This suggests that this radial effect should be taken into account by any design procedure of mixed inflow turbines with low hub-to tip-radius ratio.

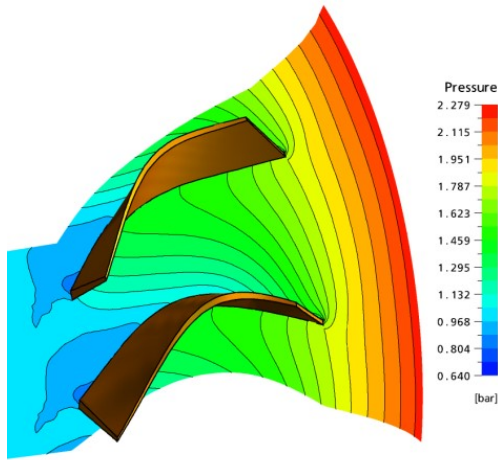


Figure 16. Pressure distribution in mid span of the blade to blade channel (Rotor with 10 blades)

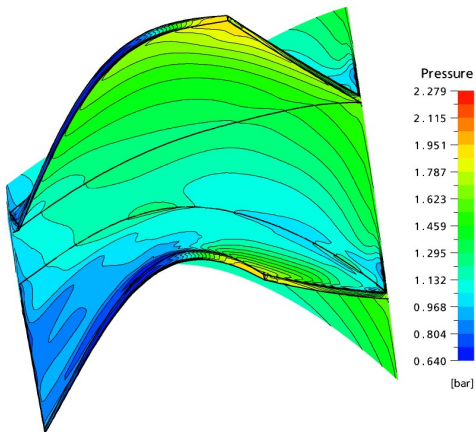


Figure 17. Pressure distribution in blade and hub (Rotor with 10 blades)

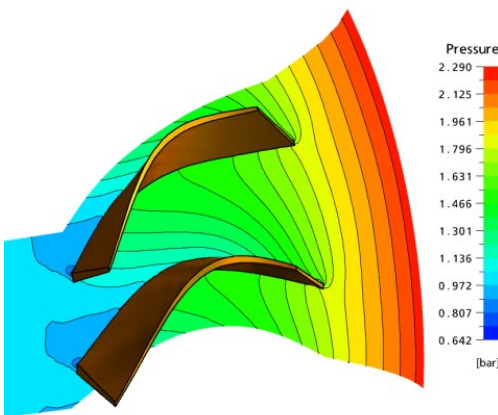


Figure 18. Pressure distribution in mid span of the blade to blade channel (Rotor with 12 blades)

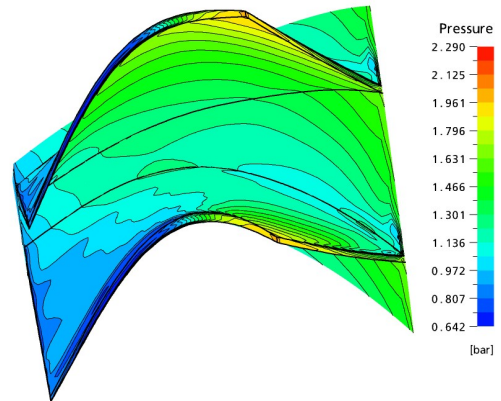


Figure 19. Pressure distribution in blade and hub (Rotor with 12 blades)

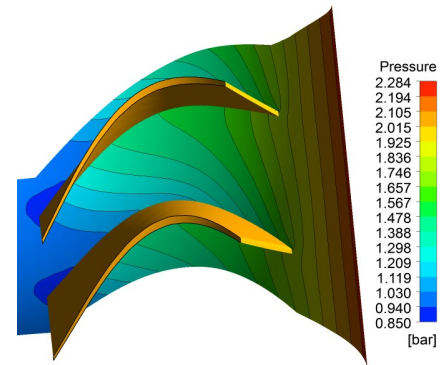


Figure 20. Pressure distribution in mid span of the blade to blade channel (Rotor with 14 blades)

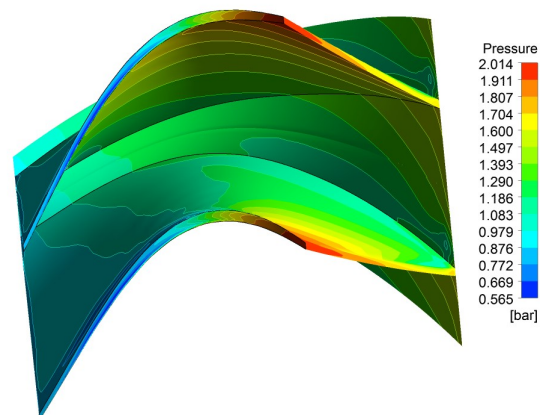


Figure 21. Pressure distribution in blade and hub (Rotor with 14 blades)

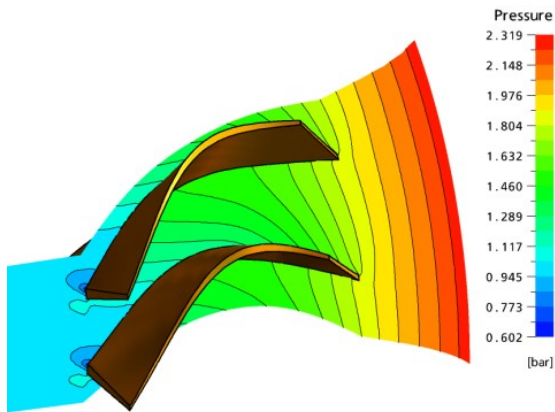


Figure 22. Pressure distribution in mid span of the blade to blade channel (Rotor with 16 blades)

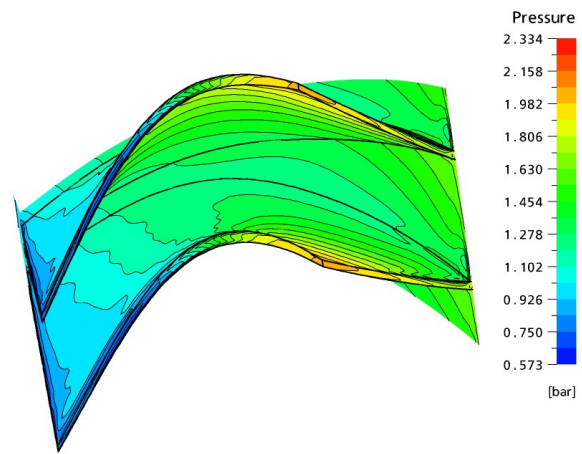


Figure 25. Pressure distribution in blade and hub (Rotor with 18 blades)

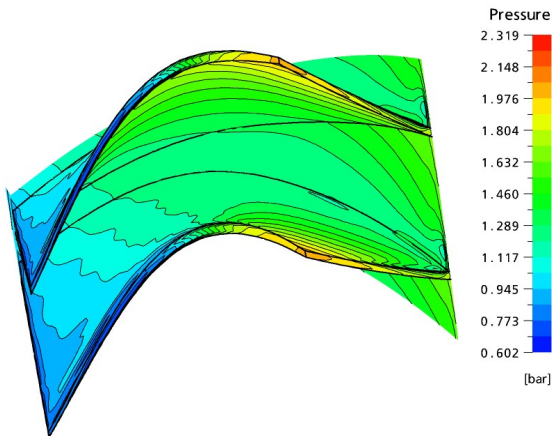


Figure 23. Pressure distribution in blade and hub (Rotor with 16 blades)

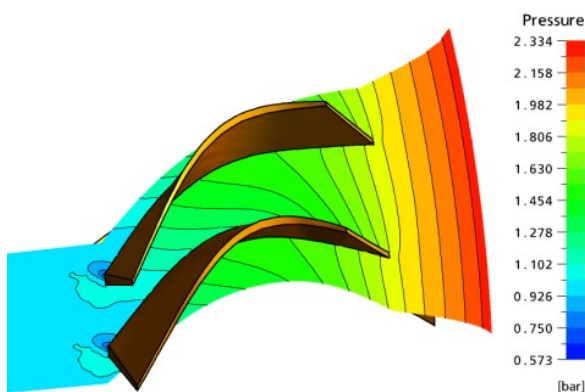


Figure 24. Pressure distribution in mid span of the blade to blade channel (Rotor with 18 blades)

Figure 26 shows the distribution of the velocity and the speed vectors in the mid span of the blade to blade channel of the rotor with 14 blades.

In this figure it is observed that the flow is well guided and accelerated towards the streamwise direction.

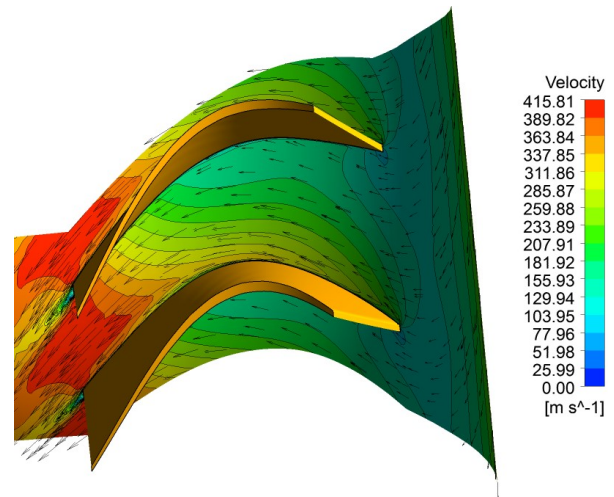


Figure 26. Velocity distribution in mid span of the blade to blade channel (Rotor with 14 blades)

The pressure distribution around the blade of the three rotors is interpreted in Fig. 27, presenting the nine blade rotor with a positive pressure gradient at the blade suction side, which produces boundary layer separation and the flow recirculation.

It can be noted that with an increase in the number of blades, the pressure difference between the two sides of the blade tends to decline, and the

recirculation zone representing a loss of energy disappears. The ideal pressure distribution seems to be the fourteen blade rotor.

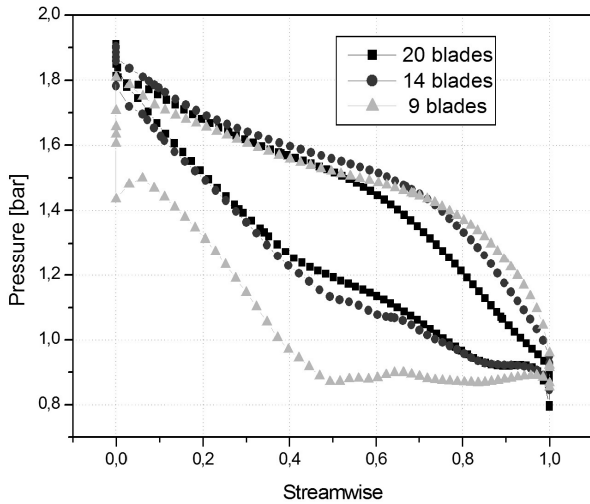


Figure 27. Variation of blade loading vs. the number of blades

3.4 Optimum rotor blade number

In order to obtain a better efficiency at these design conditions (Table 1), the geometry of the mixed inflow turbine must be optimized. Theoretical and experimental studies show that geometrical characteristics such as blade angle, axial length and number of blades have a large influence on the flow passage and the turbine efficiency. Several simulations are carried out on rotors with different number of blades (from 8 to 20) having the same geometrical shape. The results presented in Fig. 28 in terms of total to static efficiency, show that the rotor with 14 blades has the higher efficiency of about 84 % at design conditions.

The research carried out in the literature led us to compare the optimal number of blade with the one obtained using empirical formulas.

Applying Jamieson's, Glassman's, Whitfield's and Rohlik's proposed empirical formulas [17], the optimal number resulted in 27, 15, 20 and 12, blades, respectively. The closer number of blades to the present analysis is the one proposed by Glassman.

At design conditions, the mixed inflow turbine with 14 blades shows better performance. This number of blades is recommended for this turbine. When using a large number of blades, the spacing between blades is made small, the fluid then tends to receive a better guidance, but the losses due to friction will

be larger. The rotor with 14 blades offers a compromise between good guidance and minimizing losses.

Figure 29 shows the variation of the turbine total to total pressure ratio against the variation of blade number, this variation indicates the poor expansion when a low number of blades is used, resulting in a high exit losses. The torque developed by all blades is shown in Fig. 30, and the maximum torque is produced with 14 rotor blades. The torque developed by one blade is shown in Fig. 31.

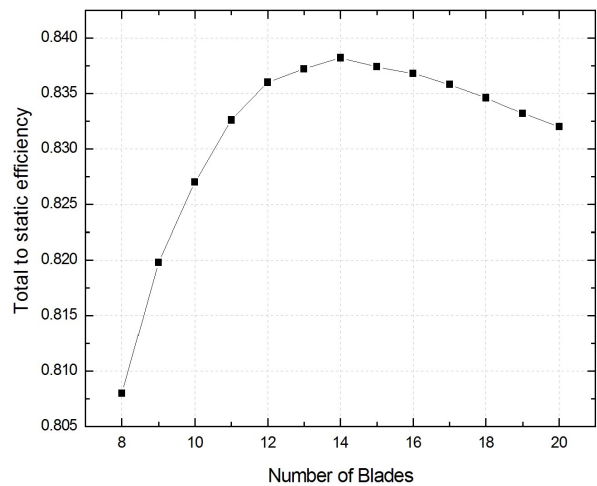


Figure 28. Total to static efficiency vs. Number of blades

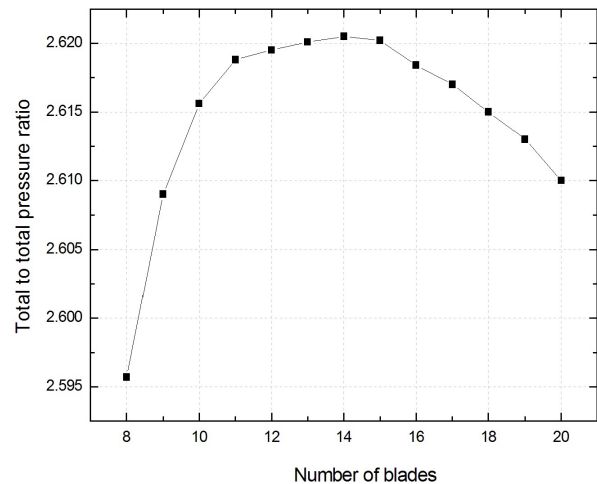


Figure 29. Pressure ratio vs. number of blades

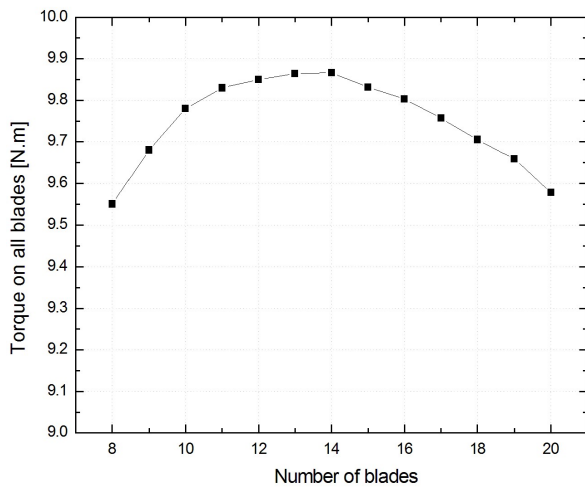


Figure 30. Torque developed by all blades vs. Number of blades

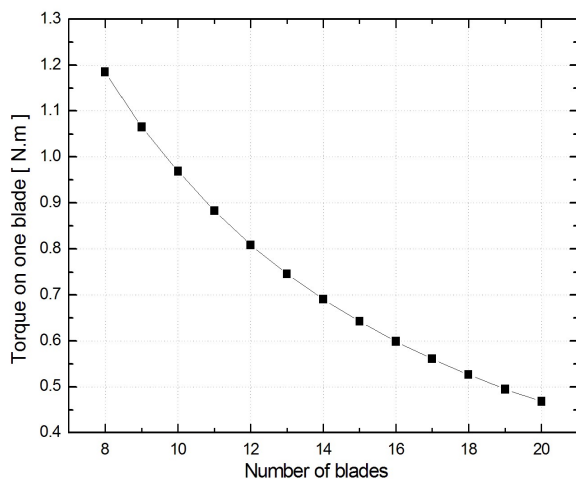


Figure 31. Torque developed by one blade

4 Conclusion

It is worth commenting that a compromise will be required to find the mixed inflow rotor performance and ultimately the most suitable number of blades. A large number of blades is desirable for avoiding reverse flow, to give better flow guidance, to distribute the available flow impulse but at the penalty of increased frictional losses, inertia, flow blockage, weight and the cost of the machine. In order to accomplish this, numerical simulations have been performed to investigate a three dimensional flow path in the rotor with a varying blade number.

It is of interest to focus on the efficiency, the power, the torque developed and the pressure ratio results. All the curves are of similar shape and present an optimum value corresponding to the number of blades, which is equal to 14. We observe that tending the blade number towards 14 will lead to an increase in all the performance parameters cited above. This might be due to a better impulse load distribution over the blades, with a minimum flow reversal effect and a better flow guidance.

Apart from this optimum value, the trends are inverted. The magnitude of all the performance variables falls, certainly due to the inertia, friction losses and the blockage effect. We might conclude from the previous discussions that the peak performance and efficiency of turbine is a compromise among definite number of blades.

References

- [1] Abidat, M.: *Design and testing of a Highly Loaded Mixed Flow Turbine*, PhD Thesis, Imperial College, London, 1991.
- [2] Abidat, M., Chen, H., Baines, N.C., Firth, M.R.: *Design of a Highly Loaded Mixed Flow Turbine*, Proceedings of the Institution of Mechanical Engineers, Part A: Journal of Power and Energy, 206 (1992), 2, 95-107.
- [3] Abidat, M., Hachemi, M., Hamidou, M. K., Baines, N. C.: *Prediction of the steady and non-steady flow performance of a highly loaded mixed flow turbine*, Proceedings of the Institution of Mechanical Engineers, Part A, Power and Energy, 212 (1998), 3, 173-184.
- [4] Arcoumanis, C., Hakeem, I., Martinez-Botas, R.F., Khezzar, L., Baines, N.C.: *Performance of a Mixed Flow Turbocharger Turbine under Pulsating Flow Conditions*, ASME, International Gas Turbine and Aeroengine Congress and Exposition, Houston Texas USA, 1995. V002T04A011.
- [5] Chen, H., Hakeem, I., Martinez-Botas, R. F.: *Modelling of a turbocharger turbine under pulsating inlet conditions*, Proceedings of the Institution of Mechanical Engineers, Part A. Power and Energy, 210 (1996), 5, 397-408.
- [6] Hamel, M., Abidat, M., Litim, S. A.: *Investigation of the mixed flow turbine performance under inlet pulsating flow*

- conditions, *Comptes Rendus Mecanique*, 340 (2012), 3, 165-176.
- [7] Karamanis, N., Martinez-Botas, R. F., Su, C. C.: *Mixed flow turbines: Inlet and exit flow under steady and pulsating conditions*, *ASME Journal of turbomachinery*, 123 (2001), 2, 359-371.
- [8] Chen, H., Abidat, M., Baines, N. C., Firth M. R.: *The effect of Blade Loading in Radial and Mixed Flow Turbines*, International Gas Turbine and Aeroengine Congress and Exposition, Cologne-Germany, 1992, V001T01A049.
- [9] Bhinder, F. S., Gulati., P. S.: *A method for predicting the performance of centripetal turbines in non-steady flow*, 1st International Conference on Turbochargers and Turbocharging, London, 1978, 233-240.
- [10] Gabette, V., San Emeterio, Ph., Arques, Ph.: *Influence d'un écoulement pulsé sur les caractéristiques de fonctionnement d'une turbine de suralimentation de moteur thermique*, *Mécanique Matériaux Electricité*, 1982, 394-395.
- [11] Dale, A., Watson, N.: *Vaneless Radial Turbocharger Turbine Performance*, 3rd International Conference on Turbocharging and Turbochargers, London, 1986, C110/86.
- [12] Chen, H., Winterbone, D. E.: *A method to predict performance of vaneless radial turbines under steady and unsteady flow conditions*, 4th International Conference on Turbochargers and Turbocharging, London, 1990, C405/008, 13-22.
- [13] Hammoud, A., Duan, Q. C., Julien, J. : *Etude de la validité de l'hypothèse de quasi-stationnarité appliquée au fonctionnement d'une turbine de suralimentation en régime pulsé*, *ENTROPIE* 29 (1993), 174-75, 79-85.
- [14] Rajoo, S., Martinez-Botas, R. F.: *Mixed flow turbine research: a review*, *ASME Journal of Turbomachinery*, 130 (2008), 4, 044001.
- [15] Khairuddin, U., Costall, A. W., Martinez-Botas, R. F.: *Influence of Geometrical Parameters on Aerodynamic Optimization of a Mixed-Flow Turbocharger Turbine*, *ASME Turbo Expo: Turbine Technical Conference and Exposition*, Montréal-Canada, 2015, V02CT42A002.
- [16] Zhang, J., Zangeneh, M.: *A 3D inverse design based multidisciplinary optimization on the radial and mixed-inflow turbines for turbochargers*, 11th International Conference on Turbochargers and Turbocharging, London, 2014, 399-410.
- [17] Dixon, S. L.: *Fluid mechanics, thermodynamics of turbomachinery*, Butterworth - Heinemann, Oxford, 1998.
- [18] Patankar, S. V., Spalding, D. B. A.: *Calculation procedure for heat, mass and momentum transfer in three-dimensional parabolic flows*, *International journal of heat and mass transfer*, 15 (1972), 10, 1778-1806.
- [19] *ANSYS CFX- Solver Theory guide*, Academic Research Release 11, ANSYS Inc., 2006.
- [20] Rhie, C. M., Chow, W. L. A.: *Numerical Study of the Turbulent Flow Past an Isolated Airfoil with Trailing Edge Separation*, *AIAA journal*, 21 (1983), 11, 1525-1532.
- [21] Pullen, K. R.: *The design and development of a small gas turbine and high speed generator*, Doctoral dissertation, Imperial College-London, 1991.
- [22] Celik, I. B., Ghia, U., Roache, P. J.: *Procedure for estimation and reporting of uncertainty due to discretization in CFD applications*, *Journal of fluids {Engineering-Transactions} of the ASME*, 130 (2008), 7, 078001.